J. Fluid Mech. (1990), *vol.* 213, *pp.* 549–571
Printed in Great Britain

Pseudo-advective relaxation to stable states of inviscid two-dimensional fluids

By G. F. CARNEVALE[1] AND G. K. VALLIS[2]

[1] Scripps Institution of Oceanography, University of California, San Diego, La Jolla, CA 92093, USA

[2] Division of Natural Sciences, University of California, Santa Cruz, Santa Cruz, CA 95064, USA

(Received 31 March 1989)

The continuous transformation of one flow into another of higher or lower energy while preserving the potential vorticity of all particles can be accomplished by advection with an artificial velocity field. Since isolated extremal energy states are stable states, this method can be used to find stable stationary flows on a prescribed isovortical sheet. A series of numerical simulations of this method for two-dimensional fluids that demonstrates its feasibility and utility is presented. Additionally, a corollary to Arnol'd's nonlinear stability theorems is discussed, which shows that there can be at most two Arnol'd stable states per isovortical sheet.

1. Introduction

In Vallis, Carnevale & Young (1989, hereafter VCY), we presented a general method for decreasing or increasing the energy of a flow while preserving the circulation on all material curves. Here we consider applications of this method to two-dimensional flows and demonstrate its utility in finding and examining stable states. Kelvin (1887) had investigated the stability of stationary flows by imagining a process analogous to the one we use. By numerical simulation of our method, we can animate the thought experiments proposed so long ago by Kelvin and extend the range of practical application of this approach based on energy extremization.

A concept which will be useful in our discussions is the isovortical sheet. Two-dimensional flow is simply the advection of vorticity (potential vorticity in geophysical contexts). Thus it preserves the potential vorticity of all material particles. A useful decomposition of phase space is achieved by grouping all the states which can be obtained from each other by a smooth, vorticity-preserving mapping or, in other words, by advection with some divergenceless but otherwise arbitrary flow field for some finite time. A trajectory in phase space must be wholly contained in such an isovortical sheet (Arnol'd 1965*a*). Furthermore, since energy is conserved in inviscid flow, any trajectory must lie on a constant-energy surface. The isovortical sheet, the constant-energy surface, and their intersection are in general all infinite-dimensional. However, if the intersection is just a point, it then follows that the state represented by that point is a stationary flow. Furthermore, if that point is a maximum or minimum of energy with respect to all isovortical perturbations in a neighbourhood of it, then it represents a stable stationary flow (cf. Arnol'd 1965*a*, *b*, 1966).

The process which we are considering moves a state point toward ever lower (or higher) energy while remaining within the same isovortical sheet. Thus it can be used

as a test for stability or a method to search for stable states in the neighbourhood (on the sheet) of any given state. The basic mechanism by which this process operates is passive advection of potential vorticity by an artificial velocity field – hence the name pseudo-advection. Since the change of the vorticity field is accomplished solely by advection, all vorticity invariants are automatically preserved. Further, the artificial convecting velocity field is adjusted at each moment so that the evolution always changes the energy monotonically. By analogy to the metallurgical process in which energy is so rapidly extracted from a material that all atomic dislocations are frozen in place, this process may also picturesquely be called 'quenching'.

An extended discussion of this method and its generalizations to all Hamiltonian systems can be found in Vallis, Carnevale & Shepherd (1989) and Shepherd (1990). Here we review the case for two-dimensional flow only. The advection of potential vorticity can be expressed in a few different useful forms:

$$\frac{\partial q}{\partial t} + \boldsymbol{v}\cdot\boldsymbol{\nabla} q = 0, \tag{1.1a}$$

$$\frac{\partial q}{\partial t} + J(\psi, q) = 0, \tag{1.1b}$$

$$\frac{\partial q}{\partial t} + \hat{\boldsymbol{z}}\cdot\boldsymbol{\nabla}\psi \times \boldsymbol{\nabla} q = 0. \tag{1.1c}$$

The velocity field, $\boldsymbol{v}$, is divergenceless and can be written in terms of a stream function, ψ. For most of our discussion the potential vorticity, q, may be left general. Some of our examples will be drawn from cases of flow over topography where the potential vorticity field is given by

$$q = \zeta + h. \tag{1.2}$$

Here $\zeta = \nabla^2\psi$ is the relative vorticity, and h is a known field independent of time. For rotating fluids, $-h(x, y)$ is the fractional change of layer depth scaled by the Coriolis parameter. The simplest case of interest is the two-dimensional Euler equation, where q is simply the relative vorticity. Note that in the form (1.1c), where $\hat{\boldsymbol{z}}$ is the unit normal vector out of the plane, it is clear that the flow will be stationary if and only if the contours of ψ and q are collinear everywhere in the domain. Thus everywhere the stationary stream function is a function of the potential vorticity, although that function may be multivalued.

In what follows, it will be assumed that all boundary integrals arising from integration by parts vanish. This will be valid in many circumstances, in particular, under the assumption of periodic boundary conditions for all fields (including h, ψ, $\boldsymbol{v}, \zeta$ and their derivatives). With such boundary conditions and the choice (1.2) for the potential vorticity, the conserved energy is the kinetic energy,

$$E = \frac{1}{2}\int |\boldsymbol{v}|^2 \,\mathrm{d}x\,\mathrm{d}y = \frac{1}{2}\int (\boldsymbol{\nabla}\psi)^2 \,\mathrm{d}x\,\mathrm{d}y. \tag{1.3}$$

States evolving according to equation (1.1) follow the contours of constant energy on the sheet. If the explicit $\boldsymbol{v}$ in (1.1) is replaced by some non-divergent but otherwise arbitrary velocity field $\tilde{\boldsymbol{v}}$, then the evolution would no longer necessarily follow the energy contours, because the diagnostic relation between the advecting velocity field and q is broken. Nevertheless, the evolution would remain on the sheet because the modified dynamics,

$$\frac{\partial q}{\partial t} + \tilde{\boldsymbol{v}}\cdot\boldsymbol{\nabla} q = 0, \tag{1.4}$$

also conserves q on all particles. If the $\tilde{v}$ can be chosen at each moment in such a way that the total energy of the fluid must change monotonically, then this equation could be used to search for energy extrema on a given isovortical sheet. One way of choosing $\tilde{v}$ to accomplish this is to take the associated stream function according to

$$\tilde{\psi} = \psi - \alpha J(\psi, q), \tag{1.5}$$

where α is an arbitrary constant. By multiplying (1.4) by ψ, integrating and using (1.5), we then obtain

$$\frac{\mathrm{d}E}{\mathrm{d}t} = \alpha \int [J(\psi, q)]^2 \,\mathrm{d}x\,\mathrm{d}y. \tag{1.6}$$

With α greater (less) than zero the energy increases (decreases) monotonically.

Now some caveats are in order. A maximum or minimum energy state on a sheet will be stable if it is isolated from other points of equal energy on the sheet. One could imagine a line of stationary states of equal energy (i.e. a ridge or valley in the energy surface). *A priori* these states are not necessarily stable because a point of the true dynamics can move along the neutral direction. The modified dynamics cannot distinguish isolated energy extrema from points on such a line, and so one cannot conclude that stability is proven simply by pseudo-advective evolution to a stationary point. One might expect that such a line of equal energy points would correspond to a symmetry of the system such as translation or rotation, and stability of any one of the points on the line might then follow from conservation of a momentum rather than a vorticity invariant. Nevertheless, it remains that convergence of pseudo-advection to a point alone does not prove stability definitively. Secondly, we note that the topology of the vorticity field is guaranteed to be conserved by the modified dynamics only for finite time. If we consider the infinite time limit, the modified dynamics can converge to a point just off the sheet (i.e. an accumulation point of the sheet) with different topological properties from the points on the sheet. This can occur by the creation of thin filaments which act to preserve the topology for any finite period but which become vanishingly thin as time goes to infinity. In our numerical examples given below, we shall see evidence of the need for these two caveats. Further discussion can be found in VCY and Carnevale & Shepherd (1989).

There are many other formulations which will accomplish isovortical and monotonic energy evolution. Powers of the Laplacian can be applied to the Jacobian term in (1.5) while maintaining the monotonicity of the energy evolution. Further variations include implicit schemes such as

$$\tilde{\psi} = \psi - \alpha(-\nabla^2)^n \frac{\partial \psi}{\partial t}. \tag{1.7}$$

A method closely related to this latter one was suggested for three-dimensional flow as a method for subgrid-scale modelling by C. Basdevant (unpublished manuscript, 1986). Numerically it is readily implemented by using iteration to approximate the time derivatives within $\tilde{\psi}$. We discussed all of these schemes in VCY. In yet another formulation that was previously unnoticed, the term ψ on the right-hand side of (1.5) may simply be dropped. That is we may take

$$\tilde{\psi} = -\alpha(-\nabla^2)^n J(\psi, q), \tag{1.8}$$

The resulting analysis is the same as previously, and in particular the energy change is monotonic.

We have performed many tests of these algorithms by numerical simulation. Comparisons among these algorithms showed that their relative efficiency in collapsing the scatter diagrams of q *vs.* ψ onto the stable state depends on the specific region of the resulting $\psi = f(q)$ curve considered and the value of the exponent n. Overall, all these algorithms behave similarly, and one or the other may be used to enhance the rate of convergence to the stable state in question. For simplicity, in all of the examples given below only the algorithm defined by (1.5) was used.

Numerical simulation is necessarily at finite resolution. This implies that the details of the small-scale motions cannot be accurately reproduced. Codes can be devised such that the enstrophy and total vorticity are conserved as accurately as desired by adjusting the time step; however, the other vorticity invariants usually cannot be so constrained. Thus with finite resolution, one does not necessarily remain on the initial isovortical sheet. A stationary flow must satisfy $\psi = F'(q) \equiv \mathrm{d}F(q)/\mathrm{d}q$. A simple variational calculation shows that these states are such that the variation of the energy vanishes when subject to the constraint that the integral $Q_F \int F(q)\,\mathrm{d}x\,\mathrm{d}y$ is fixed (where we have absorbed the Lagrange multiplier in the definition of F). Thus if the only invariants constrained during the variation are the enstrophy ($F = q^2$) and total vorticity ($F = q$) then the functional relationship between ψ and q in the extremal energy state is linear. A nonlinear relation between ψ and q corresponds to a stationary variation subject to constraints other than simply total circulation and enstrophy (cf. Bretherton & Haidvogel 1976). The importance of this point for statistical mechanics and ergodic theory has been emphasized by Carnevale & Frederiksen (1987) and Shepherd (1987). Besides the total circulation and enstrophy, the general invariants Q_F are more or less accurately conserved depending on the degree of energy build up at the highest allowed wavenumber (cf. Matthaeus & Montgomery 1981). In §3, we provide examples with resolution as low as 32×32 grid points (i.e. the maximum wavenumber equals 16 in our spectral code) that demonstrate that one can actually perform valuable experiments even at modest resolutions. The ability of simulations of pseudo-advection to reach stationary states with nonlinear q *vs.* ψ relationships demonstrates that these simulations conserve the invariants other than just enstrophy and total vorticity well enough to keep the flow nearly on the same isovortical sheet during the 'quenching' process. With sufficiently high resolution we can remain nearly on the initial sheet and so derive useful information about the sheet.

In all of the examples presented here, we have used a spectral model with periodic boundary conditions. Thus, the total potential vorticity is exactly conserved (and is identically zero), and the enstrophy is 'semiconserved', that is, is conserved as accurately as we wish depending on the choice of the size of the time step. The numerical method used here for the spatial terms is the dealiasing algorithm of Patterson & Orszag (1971). The Jacobians in (1.1*b*) and (1.5) are both dealised in this manner. The time stepping is leapfrog with frequent restarts to avoid computational instabilities. The time step must be chosen sufficiently small so that the CFL condition based on the pseudo-velocity field is satisfied. The frequency of the restart step was about every 20 time steps, which is considerably smaller than the typical values used in simulating the quasi-geostrophic equations. There may, of course, be much more efficient methods for simulating pseudo-advection; however, the current method proved adequate for the task at hand.

Recently a great deal of attention has been focused on the development of methods to distill information from potential vorticity versus stream function scatter diagrams for two-dimensional flows (cf. Read, Rhines & White 1986). When the

points in such a diagram collapse onto functional relationships the flow is in a stationary state. For non-stationary flows there is no simple functional relationship between vorticity and stream function, but it is useful to ask if the given state represented by the scattered points is in some sense near a stationary state (i.e. free mode). Verkley (1989) presents methods for explicitly incorporating information of a subset of the vorticity invariants into the search for related stationary flows. Branstator & Opsteegh (1989) have approached this problem by using a standard algorithm to minimize the squared rate of change of the given state while permitting as little distortion of the initial stream function field as possible. The drawback of that method is that the vorticity invariants are not preserved; however, an advantage is that it can find unstable stationary states. In finding stable solutions by the use of a set of dynamics which are not those obeyed by the real system our work is similar to that of Moffatt (1985). These aspects, and their relation to ideas of selective decay (cf. Matthaeus & Montgomery 1980) are discussed in VCY.

2. Implications of Arnol'd stability for the structure of phase space

There is little of a precise nature that can be said about the structure of the isovortical sheets in phase space. However, if the conditions of the stability theorems of Arnol'd (1966) are satisfied for some point, then rather strong statements can be made about the structure of phase space about that point and indeed for the entire isovortical sheet on which it lies. To put these propositions as clearly as possible, it will be useful to recapitulate some of the ideas and results of Arnol'd (1966). He provides sufficient criteria for an extreme sort of Lyapunov stability in which the associated basins of the stable points cover the entire sheet (cf. McIntyre & Shepherd 1987).

As above, we take $q = \zeta + h$ and assume all boundary integrals vanish in the following calculations. The energy is a functional of ψ given by

$$E[\psi] = \frac{1}{2}\int (\nabla\psi)^2 \,\mathrm{d}x\,\mathrm{d}y. \tag{2.1}$$

Since the evolution is simply an advection of potential vorticity, we have that the generalized enstrophy,

$$Q_F[\psi] = \int F(q)\,\mathrm{d}x\,\mathrm{d}y, \tag{2.2}$$

for any function F, is conserved.

A stationary state of the evolution equation must have the contours of q_{st} and ψ_{st} collinear; that is, there will be a functional relation between q_{st} and ψ_{st}. It is convenient to write this relationship in terms of the ordinary derivative $F'(q) \equiv \mathrm{d}F/\mathrm{d}q$ of the arbitrary function F. Thus,

$$\psi_{\mathrm{st}} = F'(q_{\mathrm{st}}). \tag{2.3}$$

Arnol'd's (1966) first stability criterion is that the function F which defines the stationary state must be such that

$$0 < c < F'' < C < \infty \tag{2.4}$$

for some choice of c and C. Under this condition a very strong statement of the stability of ψ_{st} that does not depend on the perturbations being isovortical can be given. In order to treat non-isovortical perturbations (which can have values of q outside the range of q_{st}), we extend the definition of $F(q)$. Following Arnol'd (1966) we define another function $G(q)$ which is the same as $F(q)$ for all q in the range of q_{st}.

Outside that range, G can be any function which satisfies the same condition on its second derivative as F does (i.e. inequality (2.4)). Next consider the functional

$$H_G[\psi] \equiv E[\psi] + Q_G[\psi]. \tag{2.5}$$

For any ψ this is clearly an invariant of the flow. By comparing the value of this functional for $\psi_{\rm st}$ and the perturbed field $\psi \equiv \psi_{\rm st} + \delta\psi$ one finds the following two inequalities:

$$E[\delta\psi] + \tfrac{1}{2}c \int (\delta q)^2 \,\mathrm{d}x\,\mathrm{d}y \leqslant H_G[\psi] - H_G[\psi_{\rm st}], \tag{2.6}$$

and

$$H_G[\psi] - H_G[\psi_{\rm st}] \leqslant E[\delta\psi] + \tfrac{1}{2}C \int (\delta q)^2 \,\mathrm{d}x\,\mathrm{d}y, \tag{2.7}$$

where $\delta q \equiv q - q_{\rm st}$ (cf. Arnol'd 1966, Carnevale & Frederiksen 1987). Finally by evaluating (2.6) at time t and (2.7) at the initial instant, $t = 0$, one obtains

$$E[\delta\psi] + \tfrac{1}{2}c \int (\delta q)^2 \leqslant E[\delta\psi_0] + \tfrac{1}{2}C \int (\delta q_0)^2 \,\mathrm{d}x\,\mathrm{d}y, \tag{2.8}$$

with the subscript 0 denoting the initial time. The left-hand side of (2.8) is positive definite in the perturbation and vanishes as the perturbation vanishes and thus may be used to define a norm or distance between any two functions in the phase space. (Actually the functions can disagree on a set of measure zero and still this norm would vanish.) Thus any perturbation of the state satisfying Arnol'd's criterion (2.4) must remain for all time within a distance as determined by the upper bound given in (2.8). The initial perturbed state need not be on the same isovortical sheet as $\psi_{\rm st}$. In fact, it can be anywhere in the phase space, and yet the inequality (2.8) is guaranteed to hold for all time. Not only is there a basin of stability of finite size about the stable stationary state as in nonlinear stability, but the size of the basin encompasses all of phase space.

According to (2.8), any perturbation off the sheet in the vicinity of $\psi_{\rm st}$ must remain near this point for all time even though on another sheet. This does not necessarily mean that there is a related stable stationary point (i.e. another isolated energy maximum) on the sheets close by because there could be a bifurcation to a ring of equal energy points. Nevertheless, it does imply that energy contours in the vicinity of this point but on neighbouring sheets must also remain close to this point.

One can also deduce a useful uniqueness theorem from the above inequalities (Carnevale & Frederiksen 1987). Equation (2.6) proves that the solution to $\psi = G'(q)$ where $G'' \geqslant c > 0$ is unique. To see this, assume the contrary. Let ψ and $\psi_{\rm st}$ both be solutions. Then the roles they play in (2.6) are interchangeable. The right-hand side of (2.6) is antisymmetric under interchange of ψ and $\psi_{\rm st}$, but the left-hand side is always non-negative. The only possible conclusion is that $\delta\psi$ vanishes, and hence there can be only one solution.

If one restricts attention to a particular sheet, then it can be shown that there is at most one Arnol'd stable minimum-energy state on any given sheet. If $\psi = \psi_{\rm st} + \delta\psi$ is on the same sheet as $\psi_{\rm st}$, then from (2.6) we obtain

$$E[\delta\psi] \leqslant E[\psi] - E[\psi_{\rm st}]. \tag{2.9}$$

This follows because the values of Q_G are the same for all points on the sheet (and incidentally equal to Q_F since the range of q is the same for every point on the sheet). Thus $\psi_{\rm st}$ is an isolated minimum of energy. The proof of uniqueness proceeds by considering one state to act as the perturbed form of the other, and then

interchanging their roles. The antisymmetry of the right-hand side of (2.9) implies that the difference between these states must vanish.

A similar argument can also be made with Arnol'd's second stability criterion. If

$$0 < b < -F'' < B < \infty, \tag{2.10}$$

then assuming isovortical perturbations, it follows that

$$E[\psi] - E[\psi_{\rm st}] \leqslant E[\delta\psi] - \tfrac{1}{2}b \int (\delta q)^2. \tag{2.11}$$

According to Arnol'd's second criterion nonlinear stability is proven if (2.10) holds and the right-hand side of (2.11) is negative definite. Under those circumstances the state $\psi_{\rm st}$ is in that case an isolated energy maximum. For periodic boundary conditions, the right-hand side of (2.11) becomes

$$\tfrac{1}{2}\sum_k k^2(1-bk^2)|\delta\psi|^2. \tag{2.12}$$

Thus for Arnol'd's stability in this case, we would need $b > 1$, that is, $\max \mathrm{d}\psi/\mathrm{d}q < -b < -1$.

By the same type of arguments given above there can be at most only one state satisfying Arnol'd's second stability criterion on a given sheet. Note, however, that there is nothing to preclude having one state satisfying the first criterion *and* one satisfying the second criterion (i.e. one minimum-energy and one maximum-energy Arnol'd stable state) on the same sheet.

These conclusions do not preclude the existence of other stable states, even nonlinearly stable states, which do not satisfy the Arnol'd criteria. We are being very strict in our interpretation of Arnol'd's criteria, and in obtaining the above results we have assumed that the boundary conditions on the problem are such that the integral

$$\int \nabla\cdot(\psi\nabla\delta\psi)\,\mathrm{d}x\,\mathrm{d}y \tag{2.13}$$

vanishes. This will be the case if ψ and $\delta\psi$ satisfy periodic boundary conditions, or on the infinite plane if they vanish sufficiently rapidly at infinity, or on a closed boundary if ψ is a constant and $\delta\psi$ has zero circulation. However, under more general boundary conditions exceptions to our conclusion may be found.

There is a direct connection with our results and the conclusions of Andrews (1984). A generalization of Andrews' (1984) theorem is that solutions satisfying Arnol'd's (1966) criteria must have the same symmetries as the physical specifications (i.e. boundary conditions, topography, Coriolis parameter, etc.) of the problem (see Ripa 1987). Andrews' theorem follows from the uniqueness proof given above. That is, if there is a symmetry in the problem from which one could create a family of equal-energy solutions by shifts in the symmetry direction, then the uniqueness proof would be contradicted. Thus we must conclude that a state satisfying Arnol'd's criteria cannot be used to create such a family; that is, the solution must have the symmetry in question. In the case of flow over topography, the Arnol'd stable states will have the same symmetries as the topography. For situations with no topography there is nothing to fix the phase, except perhaps other invariants which cannot be expressed as functionals of the vorticity. Thus there may be a continuum of nonlinearly stable equal-energy states with the members differentiated by the specification of another invariant not accounted for in the Arnol'd stability proof (for

further discussion see Ripa 1987; Carnevale & Shepherd 1989; Chern & Marsden 1990; Sakuma & Ghil 1990).

3. Pseudo-advection of flow over topography

Our first set of examples involves flow over topography. For an arbitrary choice of F, a solution to $\psi = F'(q)$ can be constructed if there is freedom to choose the topography. First invert this relation to write it in the form

$$q \equiv \nabla^2\psi + h = F'^{-1}(\psi). \tag{3.1}$$

Then choose ψ to be any function satisfying the relevant boundary conditions. Finally choose h to satisfy (3.1). This device is used in this section to provide the examples of nonlinearly stable flows that we wish to consider.

For our first example, we consider a stationary state satisfying

$$q_{\rm st} = \psi_{\rm st}^3. \tag{3.2}$$

For this state, we have that F'' is everywhere positive. Therefore, for an arbitrary isovortical perturbation this state must obey (2.9), which bounds the energy of the perturbation.

If the stream function satisfying this cubic relation is taken to be

$$\psi = \sin x \sin y, \tag{3.3}$$

then it follows that

$$\zeta \equiv \nabla^2\psi = -2\sin x \sin y. \tag{3.4}$$

We then choose h such that (3.2) is satisfied, giving

$$h = q - \zeta = \psi^3 + 2\psi. \tag{3.5}$$

This stable flow is illustrated in figure 1.

Next we created a non-stationary state isovortical to this stationary one by advecting it with a randomly generated static velocity field. Then we allowed the modified dynamics to act with $\alpha < 0$ (i.e. monotonically decreasing energy) to test if the unperturbed stationary state could be recovered. Depending on how poorly the vorticity invariants are conserved, the quenching may take us to a minimum energy state on a different sheet. If of all the vorticity invariants only the enstrophy is adequately conserved, then quenching would take us toward the state of minimum energy for a given enstrophy which is always such that q is a single-valued linear function of ψ. The absolute minimum energy state with the same enstrophy as this cubic state satisfies the linear relation $q = 0.645\psi$ as determined by a variational calculation (cf. Bretherton & Haidvogel 1976; Carnevale & Frederiksen 1987).

Scatter plots of q *vs.* ψ are useful in following the evolution of the flow and determining the degree to which a stationary state is reached. A non-stationary state is characterized by a scatter of points in a ψ–q plot, while a stationary state is represented by a curve since then q is a function of ψ. In figure 2, we show the q–ψ relation for the cubic state, the linear state and the scatter plot for the perturbed initial condition. The question was: toward which relation would the modified dynamics take the scattered points – $q = \psi^3$, $q = 0.645\psi$, or some other function. The resolution in this demonstration is just 32×32. Figure 3 shows the evolution of the q *vs.* ψ scatter plot as the energy is smoothly drained away, and indeed the evolution is toward the cubic relation. In the last panel the theoretical limit is drawn through the scatter points. Figure 4 shows the evolution of the q-field for this experiment.

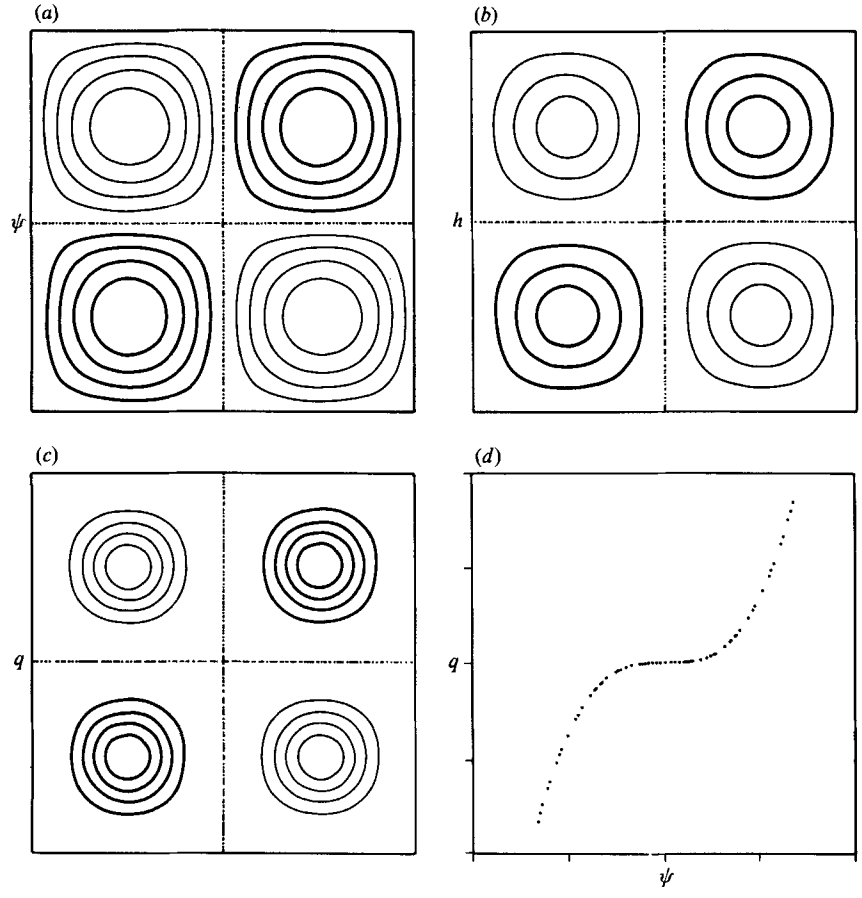

FIGURE 1 (*a–c*). Contour plots of ψ, h, and q for the unperturbed, stable, stationary state defined by $q = \psi^3$ and $h = 2\sin x \sin y + \sin^3 x \sin^3 y$. (Dark, dotted, and light contours represent positive, zero and negative values in contour plots.) (*d*) Scatter plot of q *vs.* ψ ($-1.2 \leqslant q \leqslant 1.2, -1.5 \leqslant \psi \leqslant 1.5$).

Finally, figure 5 shows that the energy asymptotes in time to the value of the unperturbed cubic state, which is considerably greater than the absolute minimum energy over all states with the same enstrophy. This demonstrates that it is feasible to use the numerical finite-resolution version of the modified dynamics to explore the phase space of two-dimensional flows.

Note that according to the discussion given in §2, the stability of a stable state with $\psi = F'(q)$ is related to the conservation of energy and $Q_F = \int F(q)\,\mathrm{d}x\,\mathrm{d}y$. In other words, the state in question can be found by extremizing E with the constancy of Q_F the only constraint. For the present example, $F'(q) = q^{\frac{1}{3}}$ and the success of the quenching must rely on the adequate conservation of the corresponding invariant $Q_F = \frac{3}{4}\int q^{\frac{4}{3}}\,\mathrm{d}x\,\mathrm{d}y$. During the quenching this quantity was constant to within better than 0.5%. Other quantities were also checked; for example, the integral of q to the eighth power was preserved with less than 1% error. These accuracies even at very low resolution are attributable to the low wavenumber of the basic state and the initial perturbations. In this simulation the amount of excitation at the highest wavenumbers does not become sufficient to create significant errors (cf. Matthaeus & Montgomery 1981).

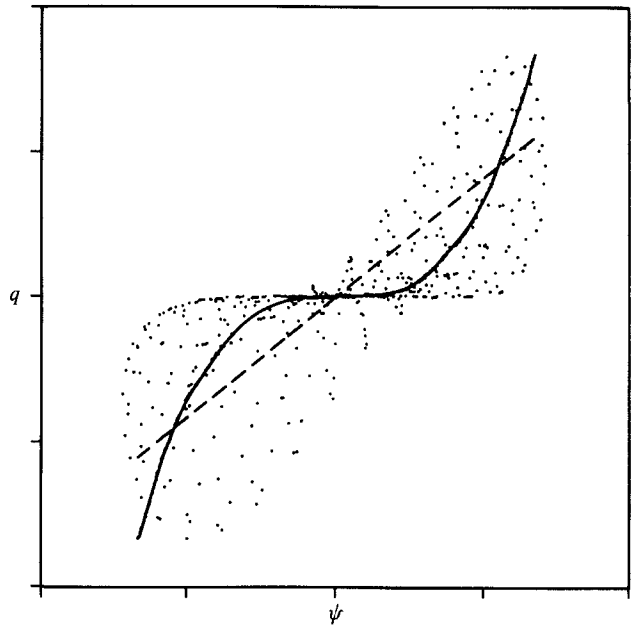

FIGURE 2. Scatter plot showing the unperturbed $q = \psi^3$ state (continous line), the randomly advected perturbed state (dots), and the state of minimum energy constrained only by enstrophy, $q = 0.645\psi$ (dashed line) (range: as in figure 1).

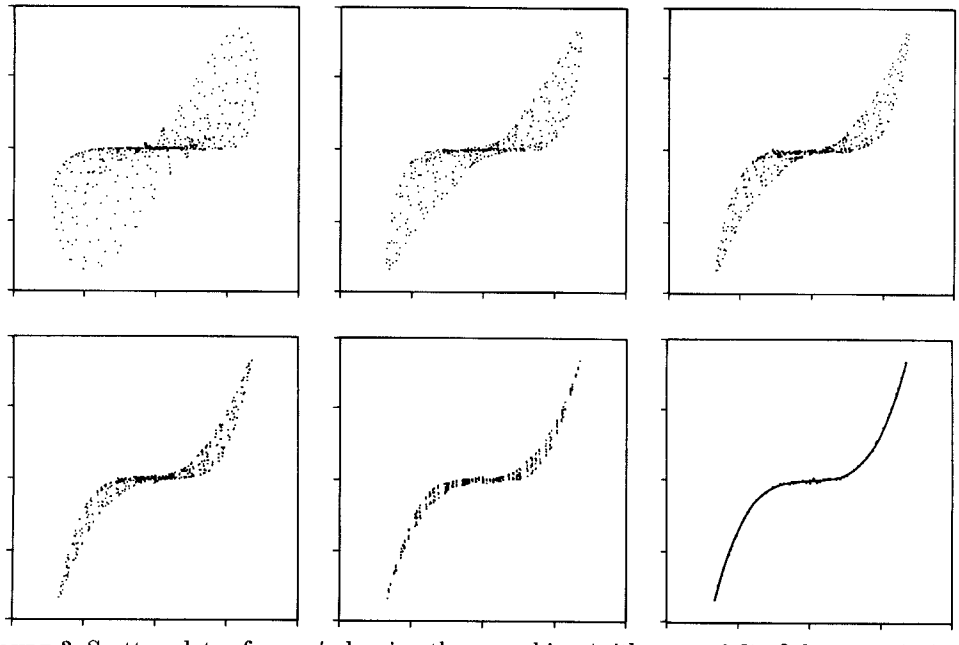

FIGURE 3. Scatter plots of q *vs.* ψ showing the quenching (with $\alpha = -0.2$) of the perturbed state back toward the unperturbed $q = \psi^3$ state (range: as in figure 1). Time proceeds left to right, top to bottom with $t = 0, 2, 4, 6, 10, 60$.

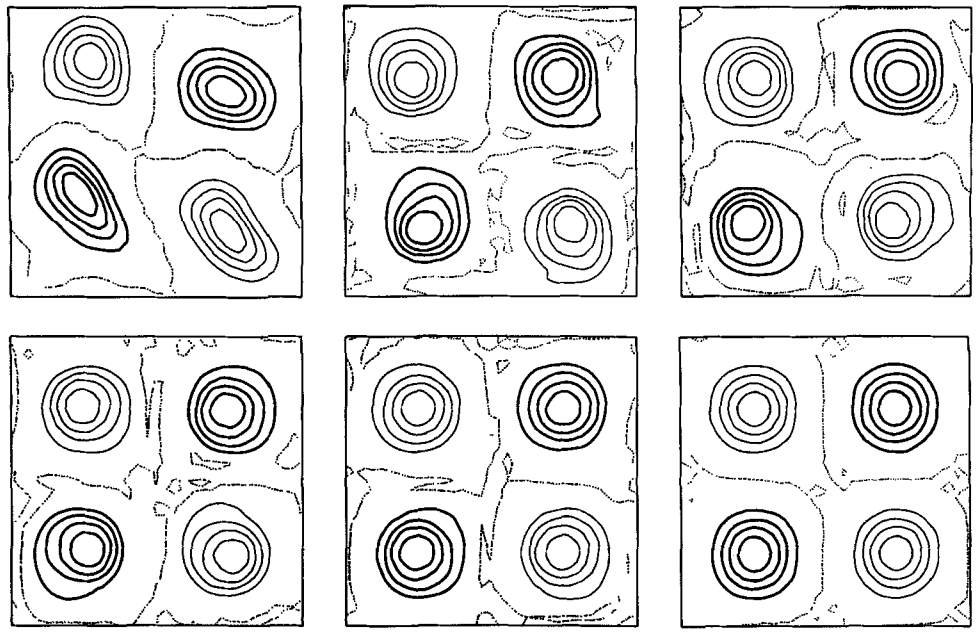

FIGURE 4. Contours of the potential vorticity field during quenching with same time sequence as in figure 3. (Contour interval 0.2; sign coded as in figure 1.)

Technically, the stationary state used in the current example does not satisfy the criteria of Arnol'd (1966) for nonlinear stability because the slope, $\mathrm{d}\psi/\mathrm{d}q$ of the q *vs.* ψ relation is infinite at a point. It is not clear what form of instability this might allow because the bound (2.6) with $c = \frac{1}{3}$ holds. Thus both the energy and enstrophy in the perturbation field are bounded by the size of the initial perturbation. What we cannot show here is that the size of this bound goes to zero as the initial perturbation energy and enstrophy become vanishingly small. In any event, the presumably nearby stable stationary state $q = \psi^3 + a\psi$ where a is a very small positive constant is essentially indistinguishable from the state with $a = 0$ for the simulation purposes, and does satisfy Arnol'd's criteria. It may be that the numerical simulation of quenching takes us to such a state on a nearby sheet and not actually to the $q = \psi^3$ state which may have a possible nonlinear instability. In fact, we have performed a series of experiments in which the initial perturbed state is taken further and further away from $q = \psi^3$ isovortically. The final state toward which the simulation relaxes is further and further from the $q = \psi^3$ state, but could be described by a state of the form $q = \psi^3 + a\psi$ with the size of a increasing with the size of the initial perturbation. We might expect that at low resolution the greater the perturbation the larger will be the deviation from the initial sheet during the perturbing and quenching processes.

We have also checked relaxation to the linear state $q = 0.645\psi$ with the same enstrophy as the cubic relation and for the same topography (3.5). This state was first perturbed by random advection to a state of higher energy, then pseudo-advection with energy decaying returned it to the linear relation. Also we have demonstrated such relaxation to the maximum energy state restricted only by that same value of the enstrophy. That state is $q = -0.392\psi$, which is Arnol'd stable ($\max \mathrm{d}\psi/\mathrm{d}q < -1$).

In further simulations of flow over topography, we tested relaxation to a variety

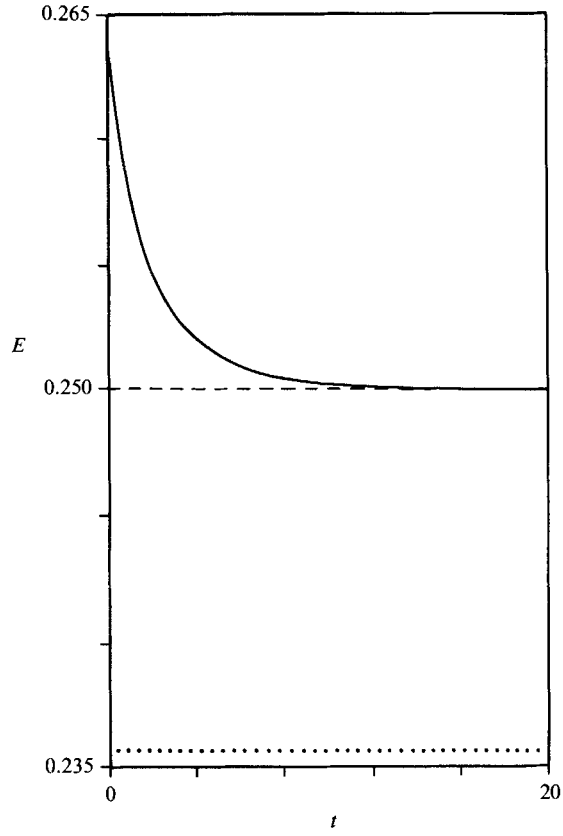

FIGURE 5. Quenching decreases the energy monotonically from the energy of the perturbed state toward its asymptotic value, which is the energy (dashed line) of the stable $q = \psi^3$ state (i.e. the minimum energy on the sheet). The minimum energy constrained only by the enstrophy, Q, in this experiment is also shown (dotted line).

of additional polynomial relationships between q and ψ of degree up to five. The results were entirely analogous to those presented above. This also included examples of increasing energy to reach maximum energy states (e.g. the Arnol'd stable $q = -0.1(\psi^3 + \psi)$).

On a sheet where there is both a maximum and a minimum energy Arnol'd stable state, it may be possible at infinite resolution to move from one to the other by pseudo-advection. In one experiment, we chose an initial condition that is an Arnol'd stable state of maximum energy. Specifically we took $\psi = -\frac{1}{2}q, \psi = \sin x \sin y$, and chose the topography accordingly. Since this is a maximum energy state, it is unstable to pseudo-advection with energy decaying. In figure 6, we show that the quenching of this state proceeds first by small-scale instability. The large-scale potential vorticity breaks up into small pieces which reassemble into a pattern of a phase opposite that of the initial condition. In this case, the flow evolves from a state of negative correlation between q and h to one of positive correlation. The final state is definitely Arnol'd stable because the slope (i.e. F'') is positive everywhere. In such cases where the intermediate states have energy dominantly at the small scales, the vorticity invariants other than enstrophy are not well conserved in the simulation (as is clear from the scatter plots and potential-vorticity contour plots). Thus this low-resolution (32×32) simulation is not accurately remaining on a given isovortical

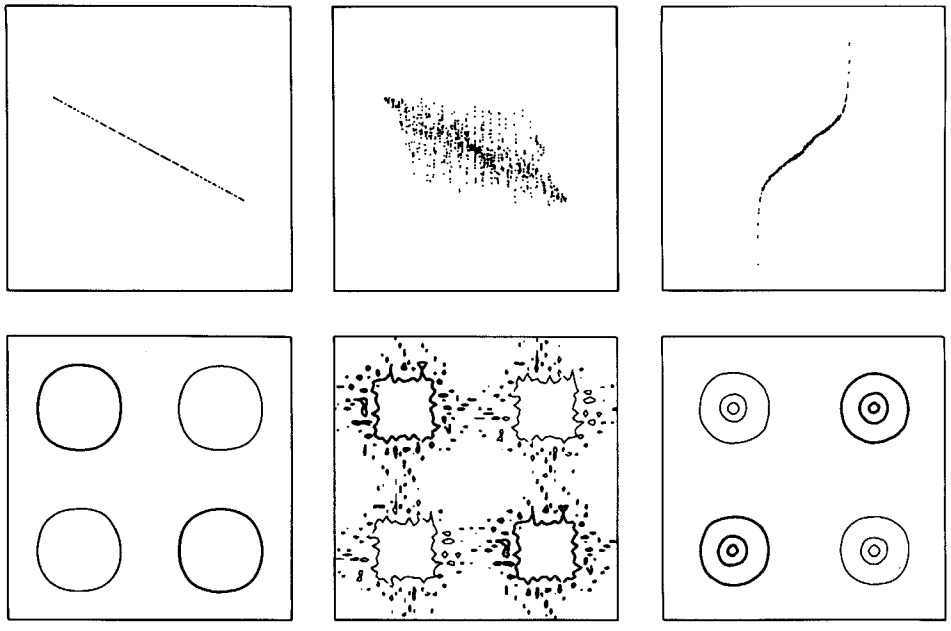

FIGURE 6. Energy is withdrawn from the maximum energy state $q = -\frac{1}{2}\psi$ by pseudo-advection (with $\alpha = -0.2$) to reach a minimum energy state. The potential vorticity contour plots (lower row) show the time sequence (left to right) with the original pattern breaking up into small parcels, which reassemble into a field anticorrelated with the initial condition. (Dark/light contours represent positive/negative values in contour plots; zero contour is not drawn; contour interval 0.25.) The q–ψ scatter plots (upper row) show the transformation from a negative slope to a positive slope state (vertical: $-1.4 \leqslant q \leqslant 1.4$, horizontal: $-1.5 \leqslant \psi \leqslant 1.5$).

sheet, but nevertheless it illustrates the concept of moving from one Arnol'd state to another.

The examples presented above were performed with unperturbed flows that occupied only the gravest mode of the box. This is not essential to the performance demonstrated, and these experiments have been repeated at higher resolution and with the unperturbed state representing a wavenumber-four flow. To emphasize that these results can be observed with basic flows at small scales, we include a case of quenching flow over an isolated mountain. In this case the unperturbed stream function has a Gaussian profile:

$$\psi = \exp(-r^2/2\sigma^2) \tag{3.6}$$

with standard deviation, σ, only 5% of the length of the side of the computational domain. For the functional relationship between ψ and q, in contrast to the previous choices of odd order, we choose a quadratic:

$$q = \psi^2 + \tfrac{1}{2}\psi. \tag{3.7}$$

Since ψ ranges from 0 to 1, the slope here is always strictly positive, and hence this flow is Arnol'd stable. Based on these choices, the underlying topography for this stable state is

$$h = \exp\left(-\frac{r^2}{\sigma^2}\right) + \frac{1}{\sigma^2}\left(\frac{\sigma^2}{2} + 2 - \frac{r^2}{\sigma^2}\right)\exp\left(-\frac{r^2}{2\sigma^2}\right). \tag{3.8}$$

Again the perturbed state is created by advection with a random but static velocity

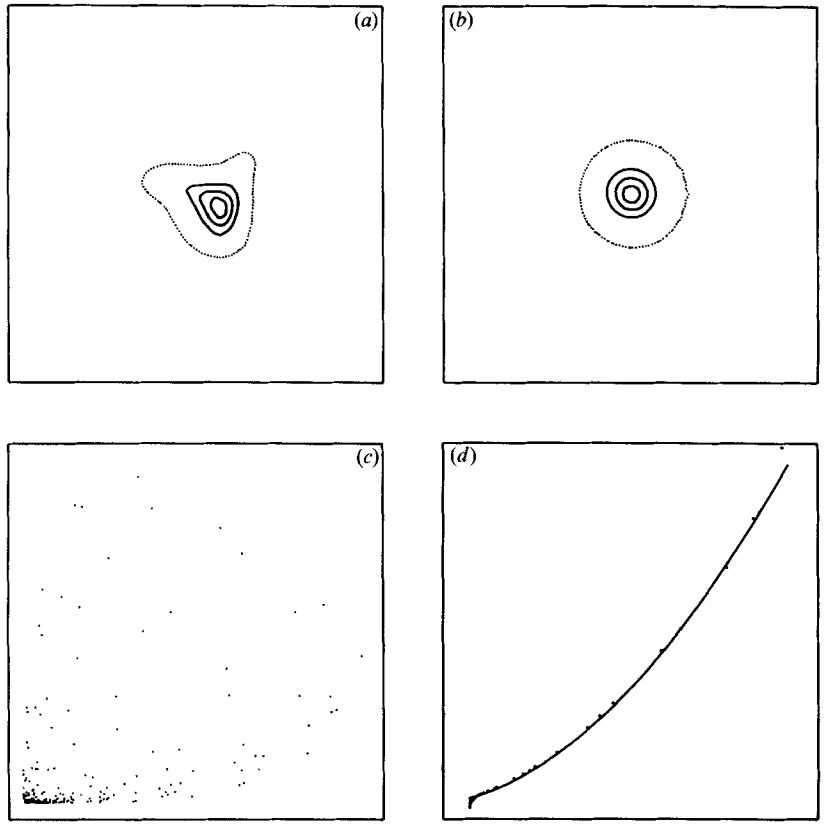

FIGURE 7. Pseudo-advection of flow over an isolated hill. (*a*) The perturbed initial-condition potential-vorticity field and (*b*) the potential vorticity after pseudo-advection back toward the minimum energy unperturbed state. (Contour interval 0.4, dotted curve corresponds to $q = 0$) (*c*, *d*) The corresponding potential q *vs.* ψ scatter plots; (*d*) also has the theoretical limit for the unperturbed state $q = \psi^2 + 0.5\psi$ as a continuous curve (vertical: $-0.1 \leqslant q \leqslant 1.6$, horizontal: $-0.1 \leqslant \psi \leqslant 1.1$).

field. The simulation was performed at resolution 64×64. The initial perturbed state and the state after a period of pseudo-advection are shown in figure 7. As the quenching proceeds the contours of q become more and more aligned with the unperturbed state. In figure 7(*b*), all but the zero contour are close to the unperturbed state (the area mean value has been subtracted from the field). The zero contour still has some noticeable distortion from a circle as is also evident from the scatter plot. Further quenching is necessary to bring all of the small q-values into alignment; however, the trend is clear. Note also that the highest q value is about 5% higher than in the unperturbed field but higher resolution and smaller time step could resolve this.

4. Pseudo-advection of vortices on a flat plane

Here we turn to the question of the pure two-dimensional problem; that is, vortices on a flat plane. For conceptual simplicity, the quenching of patches of constant vorticity is ideal and most of the explicit examples that we shall present in this section are of that type. However, this can lead to numerical difficulties in that

vorticity discontinuities are only poorly resolved in the simulations and consequently the accuracy in terms of remaining close to the original sheet has been sacrificed. In our present simulations with vorticity discontinuities, we cannot claim accurate conservation of the integrals of vorticity to high powers (i.e. about 4 and above). Nevertheless, we do claim that the phenomena illustrated are qualitatively representative of the infinite-resolution behaviour. This is confirmed in part by simulations with smoothed vorticity distributions which qualitatively demonstrate the same phenomena but with higher accuracy in terms of the conservation of the vorticity integrals. Finally, we shall end this section with an example of quenching a smoothly distributed, randomly generated vorticity field.

4.1. *Energy minimization: Kelvin's sponge*

Kelvin (1887) considered the problem of a constant vortex patch surrounded by irrotational fluid in a finite container with slip boundary conditions. Since the velocity at any point is obtained by the linear superposition of the effects of all the vorticity elements, the energy can be lowered by arranging the vorticity elements so that the velocities they contribute interfere destructively in as much of the domain as possible. We can imagine this energy minimization proceeding smoothly by producing fine filaments of vorticity whose effects tend to cancel in the region in between. The homogeneous structure of fine filaments which forms in this process Kelvin has dubbed a 'vortex sponge.' In his words 'The consumption of energy still goes on, and the way it goes on is this: the waves of shorter length are indefinitely multiplied and exalted till their crests run out into fine laminae of liquid, and those of greater length are abated. Thus a certain portion of the irrotationally revolving water becomes mingled with the central vortex column. The process goes on until what may be called a vortex sponge is formed; a mixture homogeneous on a large scale, but consisting of portions of rotational and irrotational fluid, more and more finely mixed together as time advances. The mixture is altogether analogous to the mixture of the white and yellow of an egg whipped together in the well-known culinary operation.'

For the case of periodic boundary conditions with no topography field and zero net relative vorticity, the vorticity patch is drawn into finer and finer filaments which are intermingled with the filaments of the oppositely signed background vorticity. The filamentation proceeds in such a way as to make the net vorticity in any finite subdomain ever smaller. Consequently the velocity will tend to zero everywhere. In our experiments, we confirm this intermingling of oppositely signed vorticity filaments with the energy of the flow tending to zero under quenching. At finite resolution there is actually a lower limit on the energy given by the enstrophy divided by the largest wavenumber squared, but typically this is a very small energy. Also, at finite resolution one cannot observe extremely fine filamentation because of numerical reconnection. Nevertheless, the trend toward a vortex sponge is evident in figure 8, where we start with a circular vortex patch of positive vorticity surrounded by a field of equal area and equally strong constant negative vorticity. The figure shows only the evolution of the zero-vorticity contour. In actuality, strict bimodality of the vorticity field cannot be maintained at finite resolution and a smoothed step distribution results as will be illustrated in the next section.

We have repeated this calculation with a variety of initial monopolar vortices including conical and Gaussian profiles. In each case, there is a continual tendency toward filamentation and homogenization with the energy continually decreasing. These simulations confirm the conclusions of Kelvin's (1887) thought experiment.

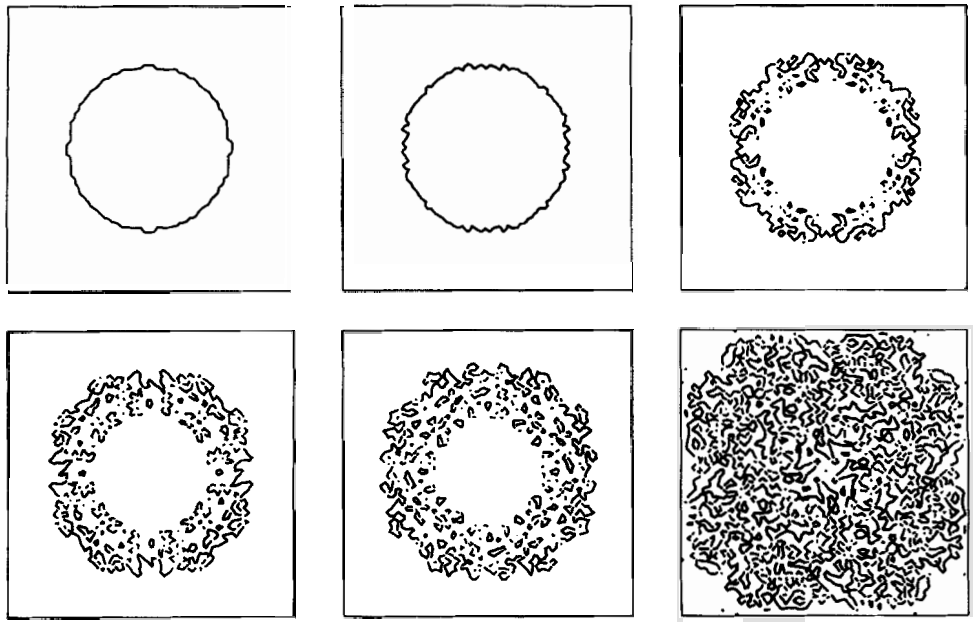

FIGURE 8. Kelvin's Sponge. Decreasing the energy of a radially symmetric vortex by quenching results in the formation of finer and finer scales. The simulations show a tendency toward complete homogenization. This is illustrated in these plots of the zero relative vorticity contour at sequential stages in the evolution (time proceeds from left to right, top to bottom).

Furthermore, they suggest that to find non-trivial stable states on the flat plane we should consider the action of increasing energy toward a maximum energy state.

4.2. *Energy maximization*

We know *a priori* that monotonic energy enhancement cannot create arbitrarily large energies because there is a bound that can be deduced from enstrophy conservation. For periodic boundary conditions in a square of side 2π, we have,

$$E = \tfrac{1}{2}\sum_{k} k^2|\psi_k|^2 \leqslant \tfrac{1}{2}\sum_{k} k^4|\psi_k|^2 = Q, \tag{4.1}$$

where the wavenumbers are integer with minimum value $k = 1$. The equality is realized only when ψ is composed solely of the gravest modes. In that case, the relationship between ψ and ζ is linear. The maximum energy achievable (i.e. on a particular sheet) will typically be lower than Q because the other vorticity invariants can restrict its value further.

The examples given below have been selected as representative of classes of basic phenomena which may be observed in the quenching process. These will aid in predicting and interpreting the outcome of quenching in more complicated situations.

Since there is no topography in these examples and nothing in the boundary conditions to fix the phase of the flow, it is clear that each case converges to a state which is part of a continuum of equal energy states. The choice of phase must be determined by information contained in the initial conditions and preserved through some invariant apart from the vortical invariants which define a sheet.

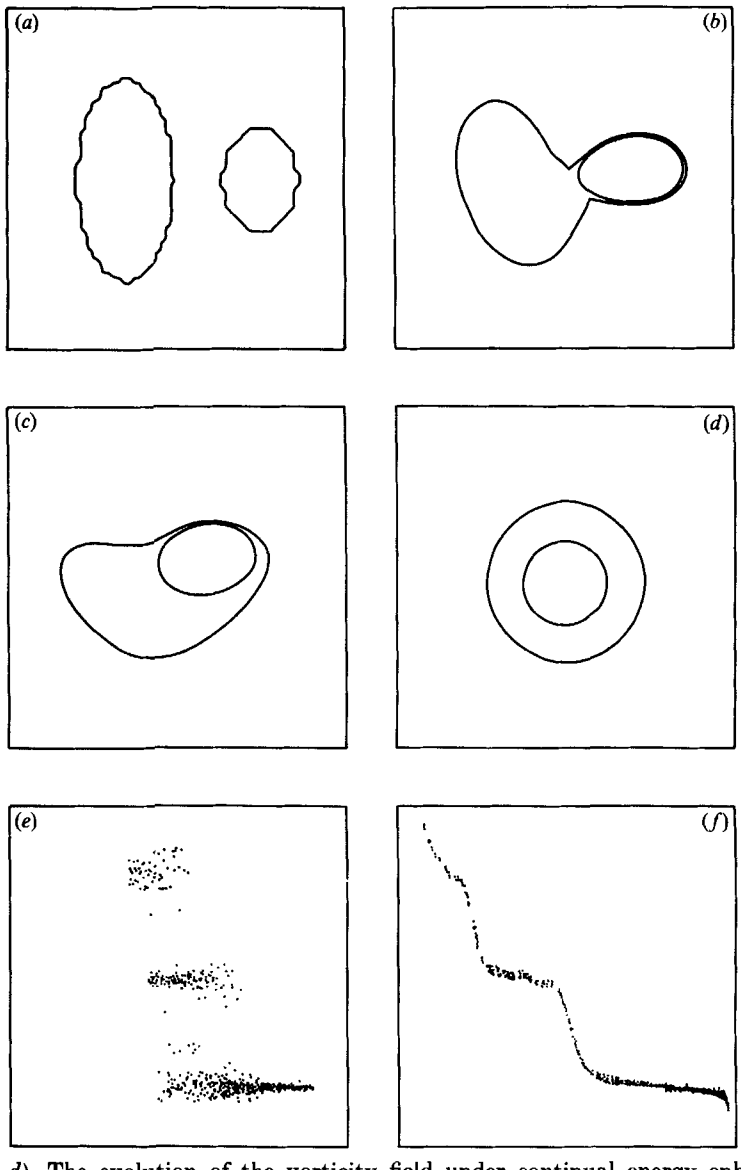

FIGURE 9 (*a–d*). The evolution of the vorticity field under continual energy enhancement by pseudo-advection of two like-signed vortex patches. The stronger vortex is engulfed by the weaker as they move to the maximum energy state of concentric circular rings of decreasing vorticity. (Contours drawn at vorticity values 0.3 and 0.6.) (*e, f*) q *vs.* ψ scatter plots for the initial and final states (vertical: $-0.4 \leqslant q \leqslant 1.2$, horizontal: $-0.7 \leqslant \psi \leqslant 0.3$).

Like-signed vortex patches

If an asymmetric vortex on a flat plane is subjected to energy increase, the flow tends to axisymmetrize. Kelvin (1887) predicted that energy enhancement will result in concentration of vorticity in concentric rings decreasing in strength from the centre. We have confirmed these predictions through numerical simulation of quenching on a variety of asymmetric-continuous and piecewise-continuous distributions of vorticity. We presented an example of this in VCY, where we took a single, simply connected, irregular patch and followed its evolution under

quenching with energy increasing. The irregular patch smoothly deforms into a circular patch as expected. The next example also shows this axisymmetrization under quenching as well as the formation of concentric rings of decreasing strength. Furthermore, the initial condition is chosen in such a way that the loss of certain topological properties will also be illustrated. We take two disjoint, like-signed, constant-vorticity patches of different strength. Under quenching with energy increasing, the vortices approach, then the weaker vortex engulfs the stronger (figure 9). The two-patch vortex then slowly axisymmetrizes reaching the final state of concentric rings with the strongest vorticity in the interior as predicted.

In spectral simulation of finite resolution (here 128×128), the vorticity of these patches cannot be strictly bimodal. The scatter plot of ζ *vs.* ψ in figure 9 shows the strong fluctuations about the intended constant-vorticity levels. During the quenching these fluctuations are redistributed to make a nearly monotonic distribution of vorticity decreasing outward from the centre of the final composite vortex. This is shown in the scatter plot at time $t = 40$ (note that the stream function increases monotonically with the radius from the centre). The thickness of the curve shown in the scatter plot would presumably continue to decrease if the quenching were continued. Another point to note is that there is a change of about 10% in the maximum value of ζ on the grid, a consequence of finite resolution.

As predicted, the presence of discontinuities (i.e. small horizontal scales) in the patch experiments makes it difficult to preserve integrals of ζ^n. In this case for $n = 4$ the variation was 4% while for $n = 8$ the variation was 30%. The time step was small enough to keep the variation of the enstrophy to within 0.2%. The important point is that the energy, which over the course of the quenching approximately doubles, asymptotes at a value more than 25% less than its maximum value predicted only from enstrophy conservation. Clearly invariants other than just the enstrophy continue to be felt even in these patch simulations.

This simulation illustrates the tendency toward a topologically inaccessible state as discussed by Moffatt (1985). Divergenceless advection cannot create, break, or destroy contours of vorticity in finite time. Therefore, during quenching at infinite resolution the topology of two disjoint patches must be maintained. Thus, ideally a thin filament cuts through the outer ring as it surrounds the inner patch. As the quenching proceeds the filament would become infinitesimally thin, and the total remaining evidence of the initial disjoint topology would be a one-dimensional line cutting through the outer ring. If the initial state had the stronger vortex actually embedded inside the weaker patch, then the final structure would be identical save for this line. Thus, in general, the $t = \infty$ states are topologically equivalent to the initial states only to the extent that the existence of such infinitesimally thin filaments is admitted. Of course, in finite-resolution simulations, once the thickness of this line is below the gridpoint separation, numerical recombination occurs, destroying the line entirely. Thus topological properties which can be maintained only through the presence of infinitesimally thin lines cannot be maintained in our simulations, and in particular in the present simulation the final state is indeed indistinguishable from the result for the stronger patch initially embedded in the weak patch. (See also figure 11 for another example of this numerical reconnection.)

Oppositely signed vortex patches

In figure 10, we show the interaction of two oppositely signed vortices as affected by quenching. Maximization of energy will require maximal separation of the vorticity of opposite sign and the concentration of vorticity of each sign with the

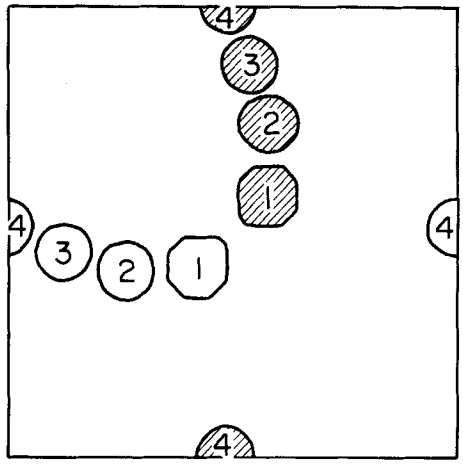

FIGURE 10. Under continual energy increase, oppositely signed vortices repel. This figure is a composite showing the relative vorticity field at four sequential points during the evolution under pseudo-advection. The shaded (white) area within each circle represents negative (positive) vorticity. The numbers 1, 2, 3, and 4 represent the times $t = 0$, 34, 80, and 292.5 respectively. Only the -0.4 and $+0.4$ contours are drawn.

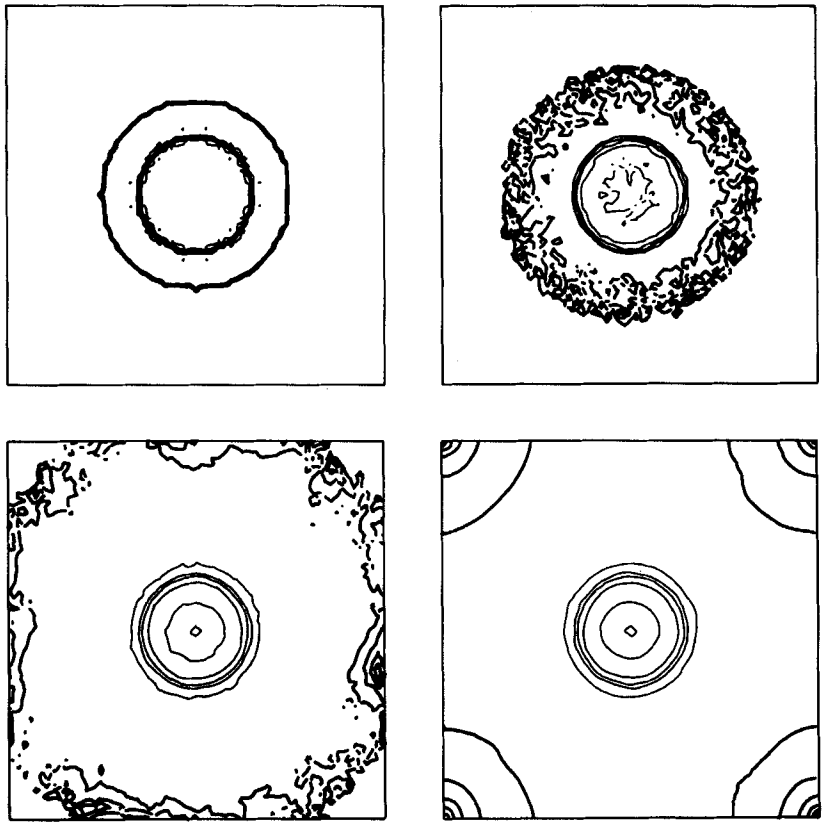

FIGURE 11. Initially a circular patch of negative vorticity is surrounded by a positive annular patch. Increasing the energy results in a maximum energy state with both circular vortices at a maximum separation. The intermediate stage shows the tendency to fine-scale filamentation. As discussed in the text the initial and final states are not topologically equivalent ($t = 0$, 1, 4.5, 30). (Contour interval 0.4; sign coded as in figure 6.)

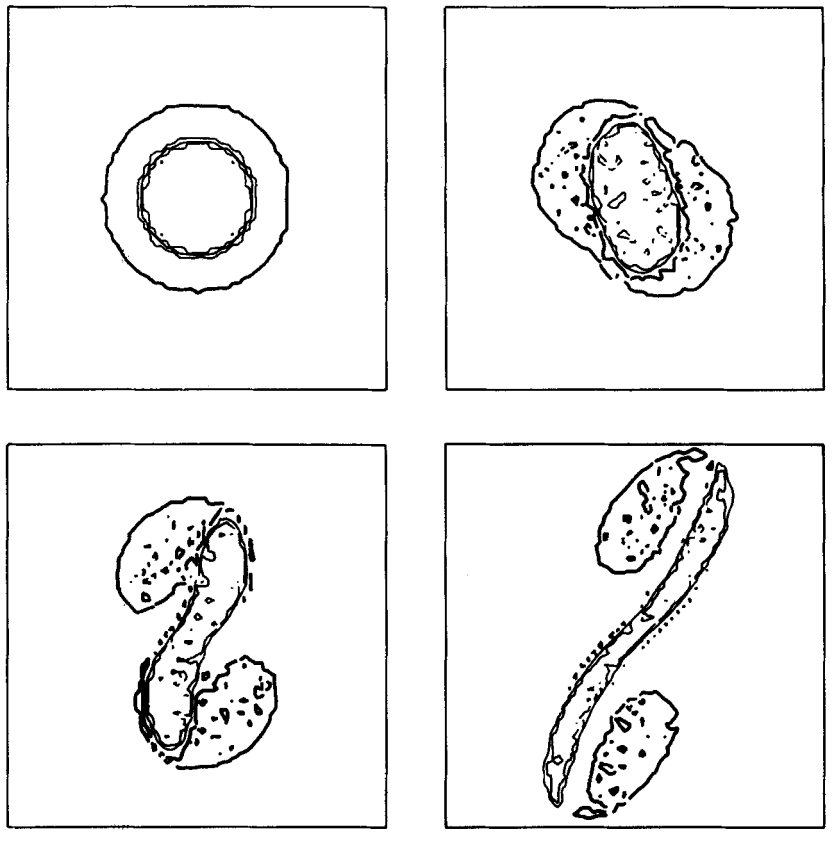

FIGURE 12. As in figure 11, except that the evolution is according to the true dynamics ($dE/dt = 0$). The annulus undergoes a double-dipole instability ($t = 0, 44, 48, 52$). Final time $t = 52$. (Contour interval 0.8; sign coded as in figure 6.)

strongest vorticity in the centre. Thus we anticipate oppositely signed vortices under quenching will repel each other and attempt to reach the largest separation possible. This tendency is clearly evident in figure 10. On an infinite plane we would anticipate the two equal but oppositely signed vortex patches to continue to separate forever, with each becoming more axially symmetric. However, in the periodic domain the repelling vortices soon fall under the influence of the vortices in the neighbouring cells, and a stable array is approached.

Concentric patches of oppositely signed vorticity

In this example, a negative circular patch is surrounded by a concentric ring of positive vorticity and the whole is on a field of zero vorticity. By the previous example, we expect the pseudo-advection will have the negative and positive vorticity repel and tend toward a state with the positive and negative vorticity regions maximally separated. In fact, this is what is observed (figure 11). The repulsion of the isotropic annulus equally in all directions results in an ablation of the annulus, which breaks into small-scale structures that then recombine to form a circular vortex maximally distant from the central negative vortex. In similar experiments where the negative core is off centre, the process appears more like an expulsion of the negative vortex rather than this isotropic ablation of the positive,

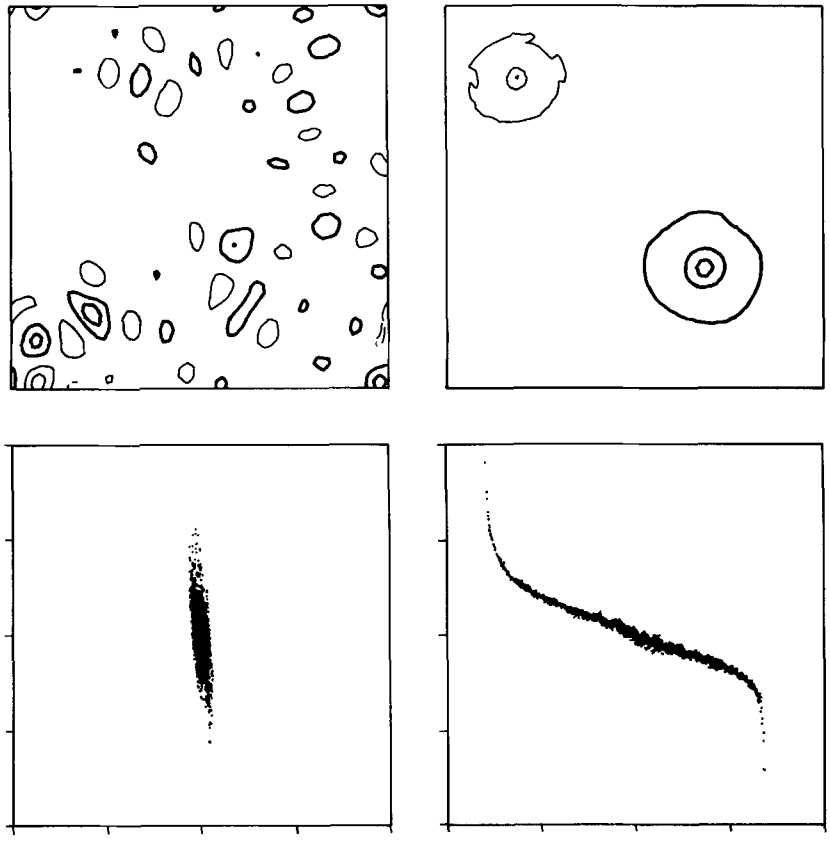

FIGURE 13. The pseudo-advection of a random initial field. The initial condition is generated with random phases and energy equipartitioned in modes with wavenumbers between 1 and 8. Continually enhancing the energy isovortically results in two large-scale eddies which do not collapse into the lowest wavenumber and have a nonlinear q–ψ relation. (Contour interval 0.8; sign coded as in figure 6.)

but nevertheless the result is the same. We emphasize that the instabilities of the modified dynamics with $\mathrm{d}E/\mathrm{d}t \neq 0$ have nothing to do with real instabilities. In figure 12, we show the evolution of the real ($\mathrm{d}E/\mathrm{d}t = 0$) instability that occurs for the same initial condition used in figure 11. This instability takes the form of double-dipole formation (Flierl 1988) and has no similarity to the ablation which occurs during quenching.

Random initial conditions

As our final example, instead of patches we use a continuous relative vorticity field. The initial field is created by equally populating all modes up to wavenumber 8 with randomly generated phases. Thus the initial vorticity contour plot primarily shows an irregular assortment of eddies of roughly wavenumber 8. From the insight formed in the patch experiments discussed above, we could anticipate that the stable configuration isovortical to this one is two large-scale monopoles of opposite sign and maximal separation. The exact form of the q–ψ relation will depend on the details of the initial vorticity distribution. As the quenching proceeds the like-signed vortices merge, the resulting large-scale monopoles do move apart to their equilibrium

positions, and the q–ψ plot shows a nonlinear relationship (figure 13). Note that if enstrophy were the only constraint during the energy increase, then the q–ψ relation would become linear and only the largest wavevectors would be exited.

5. Discussion

We have demonstrated the feasibility of numerically simulating the pseudo-advection algorithms of VCY as a means of exploring the structure of the isovortical sheets in the phase space of two-dimensional flows. A further line of investigation might be to use these algorithms in the program such as followed by Branstator & Opsteegh (1989); that is, take actual atmospheric (or other source) data for the instantaneous flow field of a non-stationary flow and apply quenching to determine whether there is a nearby stationary flow that can be identified as influencing the evolution of the given flow.

There is an obvious drawback in the algorithms investigated here. In the current formulation, pseudo-advection can lead only to stationary states. This rules out evolution toward uniformly translating or rotating form-preserving structures such as modons or rotating ellipses. Some way needs to be found to either incorporate the effects of translation and rotation into the algorithm explicitly or better still to find an algorithm which automatically determines the correct reference frame. Such a development would greatly enhance the usefulness of pseudo-advection (for a further discussion of these points, see Shepherd 1990). Also the effects of boundary conditions other than periodic need to be investigated.

We gratefully acknowledge the inspiration for this work provided by W. R. Young, and very useful discussions with T. G. Shepherd. This research has been supported by the National Science Foundation (grants OCE 86-00500 and ATM 89-14004) and the Office of Naval Research (grant N00014-89-J-1155). Additional support was provided by DARPA and ONR through University Research Initiatives N0014-86-K-0752 and N0014-86-K-0758. These simulations were performed on the Cray X-MP at the San Diego Super Computer Center.

REFERENCES

Andrews, D. G. 1984. On the existence of nonzonal flows satisfying sufficient conditions for stability. *Geophys. Astrophys. Fluid Dyn.* **28**, 243–256.

Arnol'd, V. I. 1965*a* Variational principle for three-dimensional steady-state flows of an ideal fluid. *Prikl. Math. Mech.* **29**, 846–851 [English transl. *J. Appl. Maths Mech.* **29**, 1002–1008 (1965)].

Arnol'd, V. I. 1965*b* Conditions for nonlinear stability of stationary plane curvilinear flows of ideal fluid. *Dokl. Akad. Nauk. SSSR* **162**, 975–978 [English transl. *Sov. Maths* **6**, 773–777 (1965)].

Arnol'd, V. I. 1966 On an *a priori* estimate in the theory of hydrodynamical stability. *Izv. Vyssh. Uchebn. Zaved. Matematika* **54**, 3 [English transl. *Am. Math. Soc. Transl.* **79**, 267 (1969)].

Branstator, G. & Opsteegh, J. D. 1989 Free solutions of the barotropic vorticity equation. *J. Atmos. Sci.* **46**, 1799–1841.

Bretherton, F. P. & Haidvogel, D. B. 1976 Two-dimensional turbulence above topography. *J. Fluid Mech.* **78**, 129–154.

Carnevale, G. F. & Frederiksen, J. S. 1987 Nonlinear stability and statistical mechanics of flow over topography. *J. Fluid Mech.* **175**, 157–181.

Carnevale, G. F. & Shepherd, T. G. 1989 On the interpretation of Andrews' theorem. *Geophys. Astrophys. Fluid Dyn.* (in press).

CHERN, S.-J. & MARSDEN, J. E. 1990 A note on symmetry and stability for fluid flows. *Geophys. Astrophys. Fluid Dyn.* (submitted).

FLIERL, G. R. 1988 On the instability of geostrophic vortices. *J. Fluid Mech.* **197**, 349–388.

KELVIN, LORD 1887 On the stability of steady and of periodic fluid motion. *Phil. Mag.* **23**, 459–464.

MATTHAEUS, W. H. & MONTGOMERY, D. 1980 Selective decay hypotheses at high mechanical and magnetic Reynolds numbers. In *Nonlinear Dynamics, Ann. NY Acad. Sci.* (ed. R. H. G. Hellerman), 203–222.

MATTHAEUS, W. H. & MONTGOMERY, D. 1981 Reconnection and conservation laws in MHD turbulence. In *Proc. Ninth Conf. on Numerical Simulation of Plasmas*, 30 *June–2 July*, 1980 (ed. G. Knorr & J. Denavait).

MCINTYRE, M. E. & SHEPHERD, T. G. 1987 An exact local conservation theorem for finite-amplitude disturbances to non-parallel shear flows, with remarks on Hamiltonian structure and on Arnol'd's stability theorems. *J. Fluid Mech.* **181**, 527–565.

MOFFATT, H. K. 1985 Magnetostatic equilibria and analogous Euler flows of arbitrarily complex topology. Part 1. Fundamentals. *J. Fluid Mech.* **159**, 359–378.

PATTERSON, G. S., JR. & ORSZAG, S. A. 1971 Spectral calculations of isotropic turbulence, efficient removal of aliasing interactions. *Phys. Fluids* **14**, 2538–2541.

READ, P. L., RHINES, P. B. & WHITE, A. A. 1986 Geostrophic scatter diagrams and potential vorticity dynamics. *J. Atmos. Sci.* **43**, 3226–3240.

RIPA, P. 1987 On the stability of elliptical vortex solutions of the shallow-water equations. *J. Fluid Mech.* **183**, 343–363.

SAKUMA, H. & GHIL, M. 1990 Stability of stationary barotropic modons by Lyapanov's direct method. *J. Fluid Mech.* **211**, 393–416.

SHEPHERD, T. G. 1987 Non-ergodicity of inviscid two-dimensional flow on a beta-plane and on the surface of a rotating sphere. *J. Fluid Mech.* **184**, 289–302.

SHEPHERD, T. G. 1990 A general method for finding extremal states of Hamiltonian dynamical systems, with applications to perfect fluids. *J. Fluid Mech.* **213**, 573–587.

VALLIS, G. K., CARNEVALE, G. F. & SHEPHERD, T. G. 1989 A natural method for finding stable states of Hamiltonian system. In *Proc. IUTAM conf. on Topological Fluid Dynamics Cambridge, England* 1989 (ed. H. K. Moffatt), in press.

VALLIS, G. K., CARNEVALE, G. F. & YOUNG, W. R. 1989 Extremal energy properties and construction of stable solutions of the Euler equations. *J. Fluid Mech.* **207**, 133–152 (referred to as VCY).

VERKLEY, W. T. M. 1989 On atmospheric blocking and the theory of modons. Ph.D. Thesis, Free University, Amsterdam.